2.3 AN ANALYSIS OF LIGHTNING HOLES IN A DFW SUPERCELL STORM USING TOTAL LIGHTNING AND RADAR INFORMATION

Martin J. Murphy* and Nicholas W.S. Demetriades
Vaisala Inc., Tucson, Arizona

1. INTRODUCTION

A "lightning hole" is a small region within a storm that is relatively free of in-cloud lightning activity. This feature was first discovered in severe supercell storms in Oklahoma during MEaPRS in 1998 (MacGorman *et al.* 2002). The feature was identified through high-resolution three-dimensional observations of total (in-cloud and cloud-to-ground (CG)) lightning activity by the Lightning Mapping Array (LMA; Rison *et al.* 1999). It is generally thought that lightning holes are to lightning information what the bounded weak echo region (BWER) is to radar data. That is, lightning holes are affiliated with the extremely strong updrafts unique to severe storms. The first direct association of a lightning hole with a bounded weak echo region was recently provided by Lang *et al.* (2004).

The purpose of this paper is to examine lightning holes in more detail using additional observations from another three-dimensional lightning detection system, the LDAR II at Dallas-Ft. Worth, Texas (Demetriades *et al.* 2002). These observations were taken from a set of severe hail-producing storms that passed just to the north of the DFW area on April 6, 2003 (evening of April 5 local time). One question of practical interest is whether the lightning holes can be observed at lower spatial resolution than that provided by the high-resolution 3-D observations. Another question is to what degree the lightning holes observed in these particular storms were associated with bounded weak echo regions in data from the Ft. Worth NEXRAD radar. The April 6 storms produced a number of lightning holes at fairly regular intervals. They also produced 10-cm diameter hailstones in the northern DFW metropolitan area.

2. SPATIAL-TEMPORAL REPRESENTATION OF LIGHTNING HOLES

The individual VHF radiation sources detected and located by 3-D VHF lightning systems such as LDAR II may be gridded into a simple source density-rate (e.g., number of sources/km^2/min) with various grid sizes and temporal resolutions. An additional data representation method may be obtained by first aggregating the sources according to which branch and flash produced them and then looking at the number of grid cells "touched" by the flash. This concept, which we refer to as "flash extent density" (see also Lojou and Cummins, this conference), is illustrated in Figure 1. The figure shows the branches of a flash. At each branch division, as well as at each bend or kink in any single branch, a VHF source was observed. Rather than counting all of the sources within each grid square to produce source density, we only count each grid cell once if the flash passed through it. This concept is particularly useful when storms are far from the center of the LDAR II system, where the total number of sources detected per flash is low. It also allows for a more uniform representation of storms that extend across the whole domain of the LDAR II network, including areas of low and high detection efficiency for individual VHF sources. In the remainder of this section, we will illustrate how lightning holes may be identified in both traditional source density plots and in flash extent density plots. Later analysis of the detailed 3-D structure of lightning holes will be shown using source density plots.

Figures 2 and 3 compare flash extent density and source density on a 1-by-1 km grid for a 2-minute interval from 0405-0407 UTC on April 6, 2003. In both cases, a lightning hole can be clearly observed in the western cell, which is located just to the north of Dallas. The first modification we investigate is to reduce the grid resolution. Figure 4 shows the flash extent density for the same 2-minute period computed with a 2-by-2 km grid, and Figure 5 shows the density recomputed on a 3-by-3 km grid. The lightning hole is still visible in the 2-by-2 km grid but can no longer be seen in the 3-by-3 km grid. This places an upper bound on the spatial resolution, and thus the location accuracy of the detection system, necessary for the detection of lightning holes.

In Figure 6, we again show the flash extent density on a 1-by-1 km grid but this time over a 3-minute period from 0405-0408. In this case, the lightning hole is identified somewhat more

*Corresponding author: Martin Murphy, Vaisala Inc., 2705 E. Medina Rd., Tucson, AZ 85706 USA. e-mail:martin.murphy@vaisala.com

clearly than it was in the 2-min plots. However, the storms on this day moved rapidly toward the east at about 50 km/hr. If we integrate over more than 3 min, we see the hole being covered over simply because of storm motion. The movement of the storm places an upper bound on the temporal resolution necessary in order to detect the hole.

Lightning holes are found within the convective cores of storms. By looking at either source density or flash extent density plots, it is possible to identify gaps in lightning activity that appear to be holes but are not associated with storm cores. To remedy this problem, we may look for lightning holes by taking into account that the storm cores are also the region where flashes typically initiate. Therefore, if we represent not only the source or flash extent density but also some information about flash initiation locations, we can eliminate spurious lightning holes. This procedure is illustrated in Figures 7 and 8. Figure 7 shows a simple source density plot without any information about flash initiation locations. Two possible holes are seen, one in the western supercell and one between the western and central cells. Only the higher values of source density within the western cell provide a clue that the hole within that cell is the real hole. Figure 8 incorporates flash initiation information. The color scale for this source density plot is based on the red-green color scale used in NEXRAD velocity images. In this case, green is used for grid cells that contain no flash initiation sources, and red is used for those cells that do contain flash initiation sources. The density scale is the same for both red and green. All source densities less than 8 sources/km^2 over the 2-minute interval are plotted in gray, and above that value, the color changes correspond to densities of 16, 32, 48, 64, and 128 sources/ km^2. In this image, we clearly see that the true lightning hole in the western cell is surrounded by a ring of higher source densities that also include the initiation points of flashes, while the spurious hole between cells not only is surrounded by lower overall densities but does not have any nearby flash initiation points.

3. LIGHTNING HOLES IN THE APRIL 6 SUPERCELLS AND THEIR RELATION TO RADAR INFORMATION

A cyclical behavior of lightning hole evolution was observed many times in the April 6 supercell storms. A representative example of one of these cycles is shown in Figures 9 a-d, which show a sequence of four source density plots covering a period of about 15 minutes. In this sequence, we see a lightning hole open up closer to the southeast side of the western supercell (a), become a dominant feature of the cell (b), and then open up again on the western side of the cell (c) shortly before another hole begins to form on the southeast side of the cell (d). Approximately the same periodicity applies to series of VHF lightning sources that rise up from the tops of storms. These series have been associated with overshooting tops and "convective surges" by Hamlin and Harlin (2002) and MacGorman *et al.* (2002). The observation of cyclical lightning hole evolution in these supercells further suggests that the holes are associated with strong updrafts.

A robust test of the association of lightning holes with strong updrafts is their relationship to bounded weak echo regions as observed by radar. One such example was presented by Lang et al. (2004). In the remainder of this analysis, we present a comparison of lightning holes with volumetric radar data from the NEXRAD radar at Ft. Worth.

Figure 10a shows a VHF source density plot in which we have marked the location of the lightning hole with a yello diamond. Figure 10b shows the corresponding base reflectivity image. We can investigate the full structure of the lightning hole by expanding Figures 10a-b into three dimensions, as shown in Figs 10c-d. Figure 10c shows all of the tilts of the radar volume scan geolocated in three dimensions (latitude, longitude, altitude). The altitude axis has been expanded for easier viewing, and the lightning hole position has been marked with a vertical black bar. Figure 10d shows a similar plot but for the lightning source densities in vertical layers of 1 km thickness. The time period of the lightning analysis is 04:04-04:06 UTC, and the radar volume scan was taken between 04:05-04:10 UTC.

In the 3-D radar analysis in Fig 10 c, we find that there is no single, continuous bounded weak echo region as was observed at mid-altitudes by Lang *et al.* (2004). Rather, we find that the weak echo region along the southeast flank of the storm extends to an altitude of approximately 6-7 km, and that there is another notch in the echo structure along the western part of the cell at altitudes from about 5 km up. At middle levels (5-7 km), where both weak echo areas are seen, the reflectivity pattern takes on a sideways S shape. Contrast this structure with the lightning hole in Fig. 10 d. In that plot, which summarizes in 3-D the individual slices that we have studied, the body of the lightning hole is primarily seen between

6-10 km altitude but also can be observed to some degree at altitudes as low as 3 km. We also note, however, that the entire lightning hole is not well observed at any single altitude. Rather, we find that at lower altitudes (e.g., below 6 km), the highest source densities (blue-green) are observed on the north and southwest sides of the hole. At middle altitudes (6-8 km), source densities are somewhat higher and the highest values begin to wrap around to the east and southeast of the hole position. At altitudes above 9 km, the highest source densities (yellow-red) are found on the south and east sides of the hole. Thus, the lightning hole in this DFW storm is not really a single feature associated with a single radar feature but rather a convenient 2-D feature that captures the vertical integration of a more complex structure.

Comparing the radar and lightning structures, we find that lower level precipitation, located mainly on the north and west sides of the lower-altitude weak echo region, is coincident with the low-level lightning activity. Likewise, upper level precipitation, which is mainly south and east of the upper-level weak echo notch, is coincident with the dominant high-altitude lightning activity. Thus the low-level and upper-level parts of the lightning hole are associated with weak echo regions as observed by radar. In the central portion of the lightning hole, however, there is significant mid-level precipitation in the middle of the S-shaped reflectivity profiles that is not associated with any lightning activity. The lightning activity at those altitudes is located in precipitation along the north side of the S-shaped reflectivity profile.

4. DISCUSSION

Our two main observations of lightning holes in the April 6, 2003, supercells are that (1) the lightning holes underwent cyclical development and decay, and (2) they were not linked to a bounded weak echo region but rather were a manifestation of a more complicated radar structure. The complete lightning hole was often only observable through a 2-D projection of the complete 3-D structure of the lightning activity. Thus, while full 3-D total lightning data is very useful for understanding the structure, the implication is that 2-D data with location accuracy at least as good as 1-2 km and a number of events in each flash are sufficient for operational use, at least as far as lightning hole observations are concerned.

The main question regarding the cyclical development of lightning holes is whether this development truly provides a window into the development of updrafts and the timing of severe weather. Some storms with supercell characteristics have been observed to have discrete updraft cycles (Weaver and Nelson, 1982; Nelson and Knight, 1987) as opposed to a steady updraft as the classical conceptual model of a supercell indicates. The cycling of updrafts noted in the literature has a periodicity on the order of 10 min. Our lightning hole periodicity of approximately 15 min is consistent with this value. In terms of specific evidence that lightning hole cycles were tied directly to updraft cycles, we searched for “convective surges” in the lightning activity but were unable to identify any. A possible reason for this is that the April 6 supercells developed into very dry air at middle and upper levels (Fig. 11). The entrainment of this very dry air may have prevented updrafts from penetrating to very high altitudes. We also looked for evidence of updraft cycles by examining the low-level radial velocity data from the Ft. Worth NEXRAD. Although we did not have multiple doppler capability, we did find what appeared to be a cyclical behavior in both the strength of the mesocyclone and the convergence near the weak echo region at low altitudes.

In our case, the lightning holes were not associated with a bounded weak echo region but rather were only observable as the result of doing a 2-D projection of the entire vertical structure, which was more complex. At altitudes mainly between 3-5 km, the lightning-free region was clearly associated with the weak echo region. At altitudes above 9 km, the lightning-free area was associated with another weak echo notch on the northwest side of the storm. This weak echo notch may simply have been due to the way the strong shear organized the upper-level precipitation. The most interesting finding was at middle altitudes (5-7 km), where the center of the lightning hole was filled with significant reflectivity. This finding is potentially similar to observations of the 29 June 2000 STEPS supercell above 9 km shown by Lang *et al.* (2004). They showed much higher reflectivity overlaying the bounded weak echo region in that storm, but that higher reflectivity area was still associated with the lightning hole. One possible explanation lies in recent findings by Scharfenburg *et al.* (2004). Using differential reflectivity measurements from a dual-polarization radar, they showed that supercooled raindrops can reach altitudes of several km above the local freezing level in supercell storms. Given that the April 6 storms

were significant hail producers, it is also very possible that the high reflectivity area in the center of the lightning hole was due to hail in wet growth conditions. Either explanation would preclude non-inductive charge separation in that part of the storm.

Finally, it is important to note that, as in studies using the LMA, we have so far only observed lightning holes in severe thunderstorms. Therefore, despite some of the uncertainties, we conclude that lightning holes are important features that happen to be easy to identify in 2-D projections of total lightning information. They are probably indicative of severe weather regardless of their direct link to a bounded weak echo region. We have presented at least some evidence that cycles of lightning holes may be directly related to cycles in the updraft. Future work should seek to establish a clearer link to updrafts through multiple-doppler analysis. As well, dual-polarization radar may be used to investigate the nature of the precipitation found in the center of lightning holes such as the ones shown in this paper. Model studies that include detailed microphysics, electrification, and lightning may also be used to clarify the relationship of lightning holes to storm dynamics and microphysics.

REFERENCES

Demetriades, N.W.S., M.J. Murphy, and K.L. Cummins, 2002: Early results from the Global Atmospherics, Inc., Dallas-Fort Worth Lightning Detection and Ranging (LDAR II) research network. 6th Conf. on Integrated Observing Systems, Amer. Meteorol. Soc., Orlando, FL, 202-209.

Hamlin, T. and J. Harlin, 2002: Tornado signatures and precursor activity from 3-D lightning mapping observations. 21st Conf. on Severe Local Storms, Amer. Meteorol. Soc., San Antonio, TX, 435-437.

Lang, T. *et al.*, 2004: The Severe Thunderstorm Electrification and Precipitation Study. *Bull. Amer. Meteorol. Soc.*, **85**, 1107-1125.

Lojou, J.-Y. and K.L. Cummins, 2005: On the representation of two- and three-dimensional total lightning information. Paper 2.4, this conference.

MacGorman, D., D. Rust, O. van der Velde, M. Askelson, P. Krehbiel, R. Thomas, B. Rison, T. Hamlin, and J. Harlin, 2002: Lightning relative to precipitation and tornadoes in a supercell storm during MEaPRS. 21st Conf. on Severe Local Storms, Amer. Meteorol. Soc., San Antonio, TX, 423-426.

Nelson, S.P. and N.C. Knight, 1987: The hybrid multicellular-supercellular storm: An efficient hail producer. Part I: An archetypal example. *J. Atmos. Sci.*, **44**, 1942-1959.

Rison, W., R.J. Thomas, P.R. Krehbiel, T. Hamlin, and J. Harlin, 1999: A GPS-based three-dimensional lightning mapping system: Initial observations in central New Mexico. *Geophys. Res. Lett.*, **25**, 3573-3576.

Scharfenberg, K., P.T. Schlatter, D.J. Miller, and C.A. Whittier, 2004: The use of the "Z_{dr} column" signature in short-term thunderstorm forecasts, 11th Conf. on Aviation, Range, and Aerospace Meteor., Amer. Meteorol. Soc., Hyannis, MA, paper P5.5 (CD-ROM)

Weaver, J.F. and S.P. Nelson, 1982: Multiscale aspects of thunderstorm gust fronts and their effects on subsequent storm development. *Mon. Wea. Rev.*, **110**, 707-718.

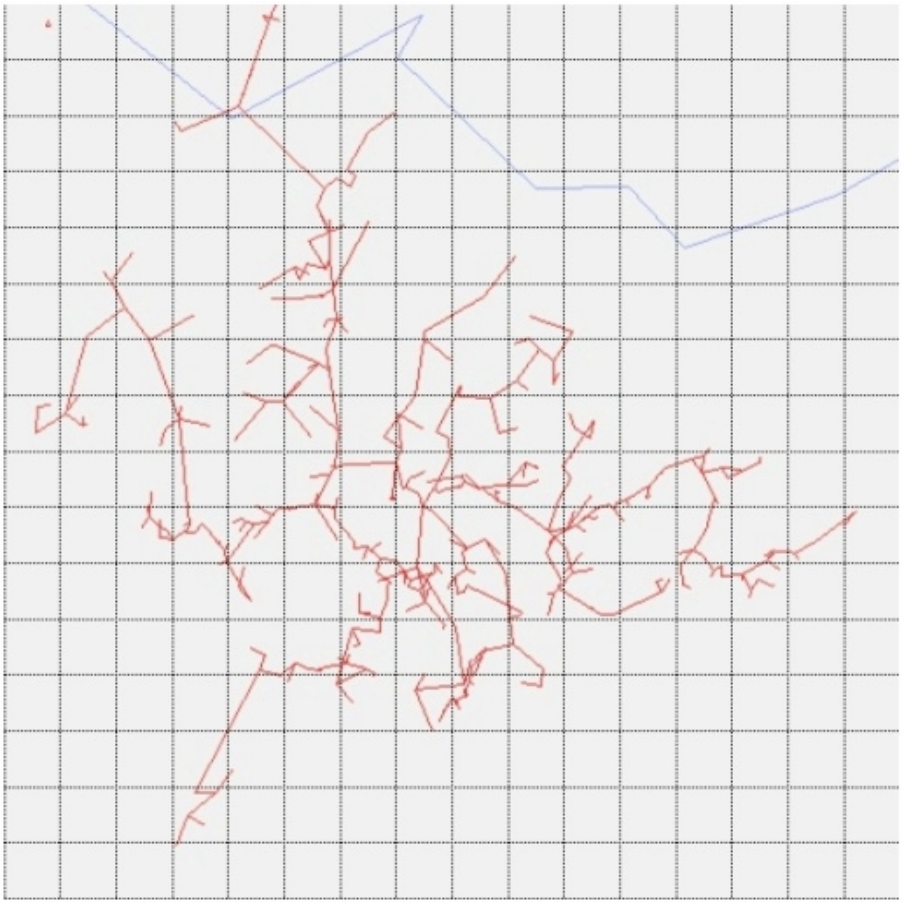

Fig. 1. Concept of flash extent density (see also Lojou and Cummins, this conference). VHF sources have been connected by lines to form branches, and a grid has been established over the area. Regardless of the number of branches or sources, each grid cell that is touched by one or more branches is counted once for this flash.

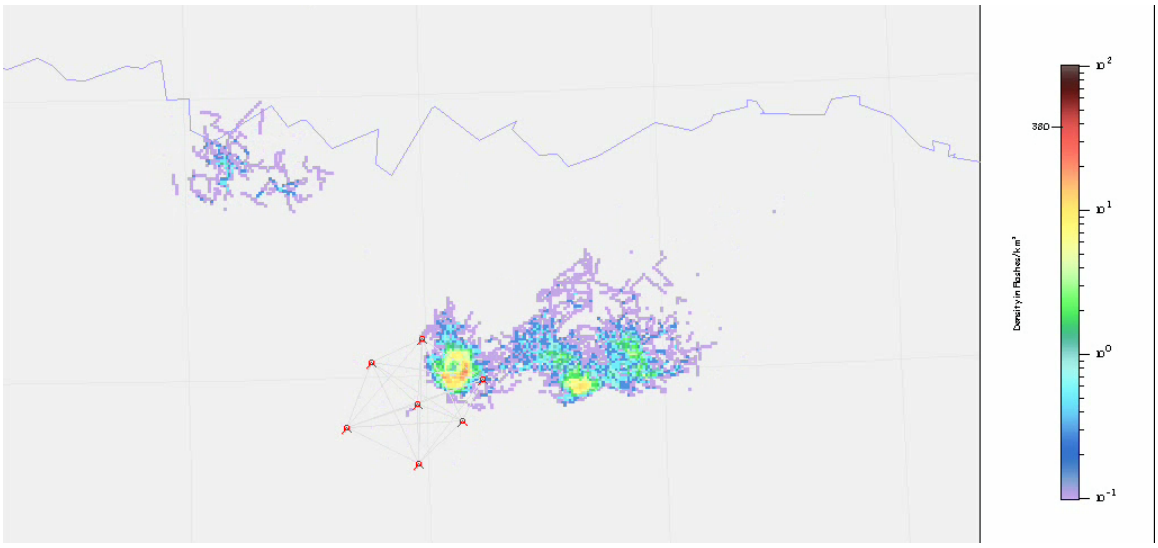

Fig. 2. Flash extent density from 0405-0407Z on April 6, 2003 using a 1X1 km grid resolution.

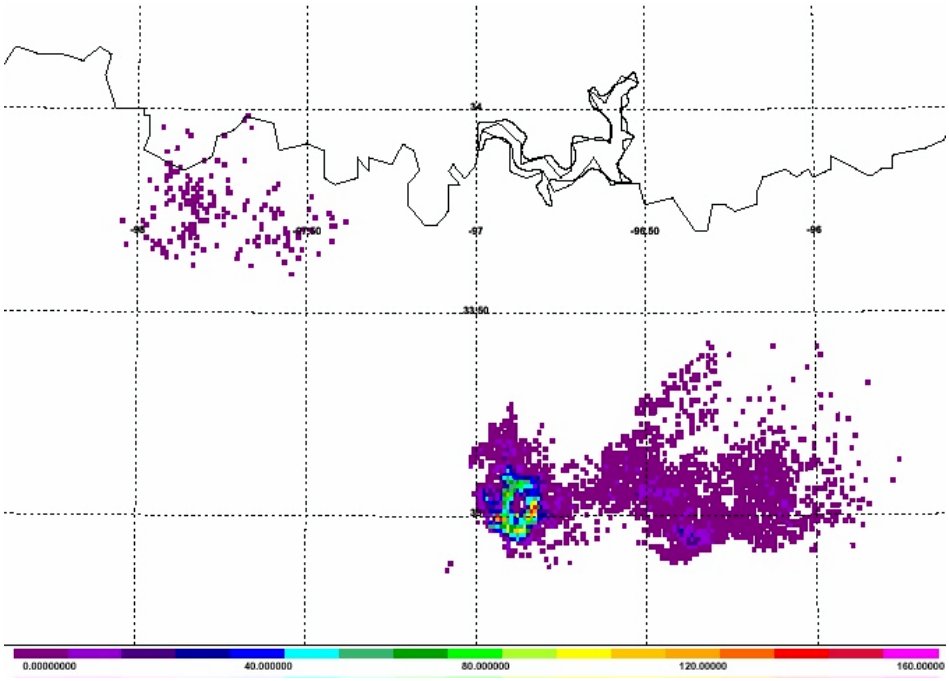

Fig 3. VHF source density from 0405-0407 Z, April 6, 2003, using 1X1 km grid resolution.

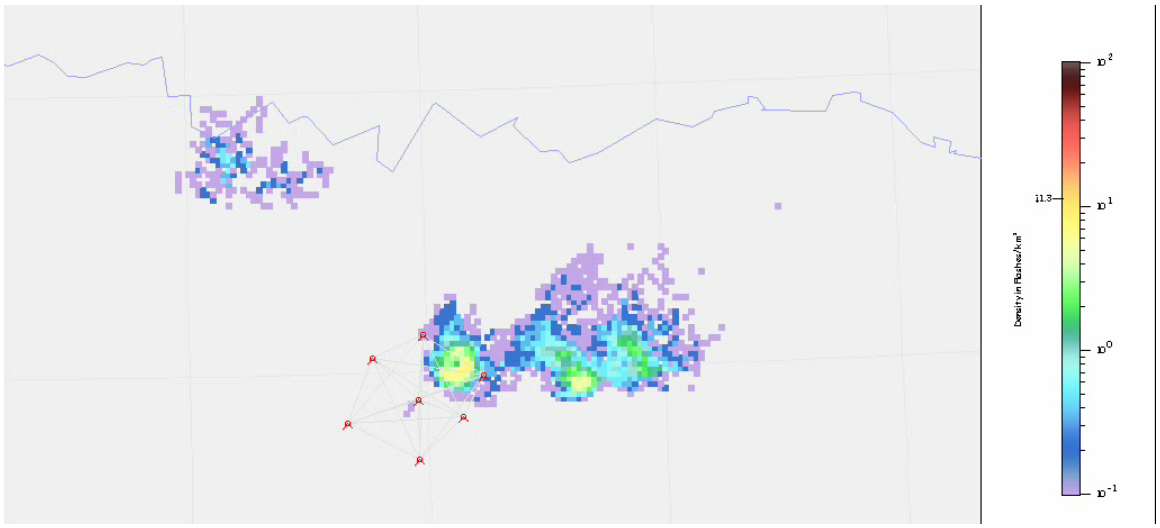

Fig. 4. Flash extent density for 0405-0407 on a 2X2 km grid.

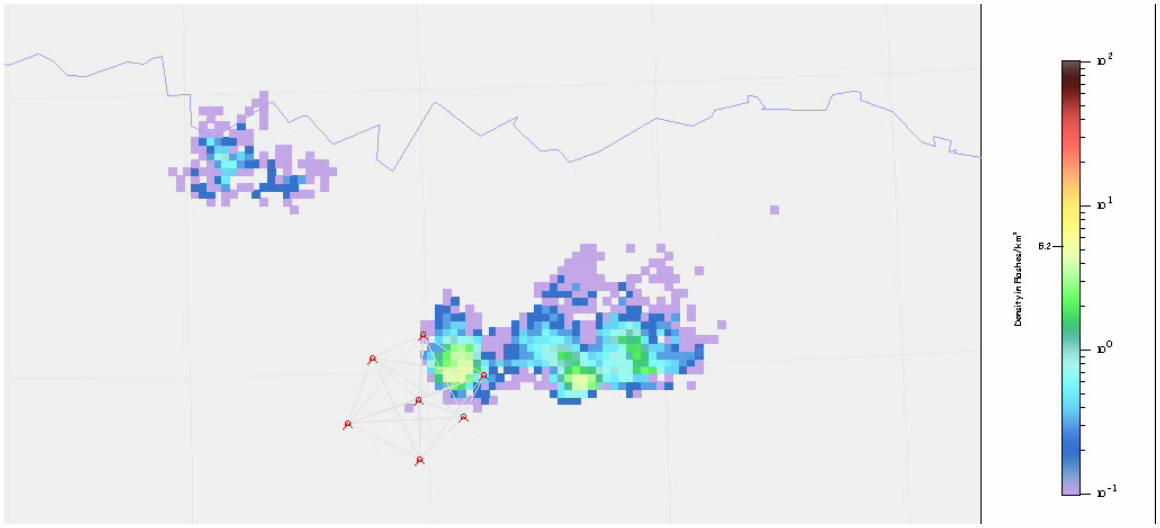

Fig. 5. Flash extent density for 0405-0407 on a 3X3 km grid.

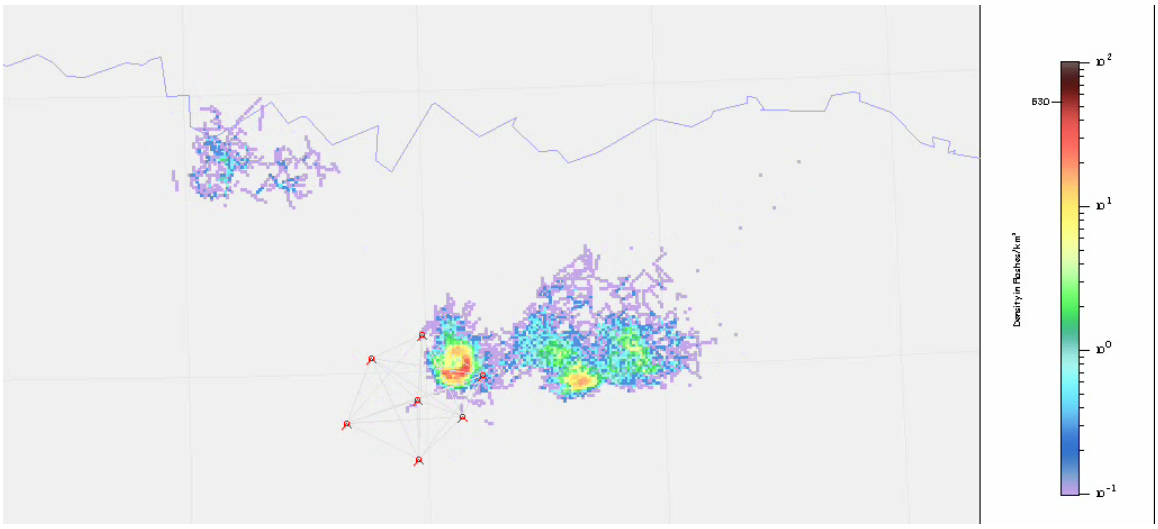

Fig. 6. Flash extent density for a 3-minute period (0405-0408) using a 1X1 km grid.

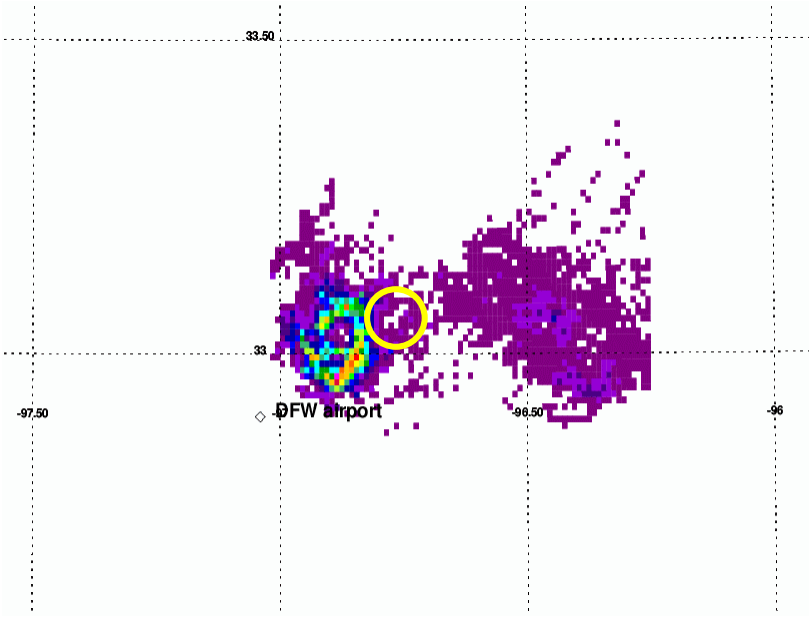

Fig. 7. Source density for 0404-0406 Z on a 1X1 km grid. Main lightning hole is just northeast of DFW airport. A spurious hole (circled) is seen to the ENE of the main hole in an area of lower source density.

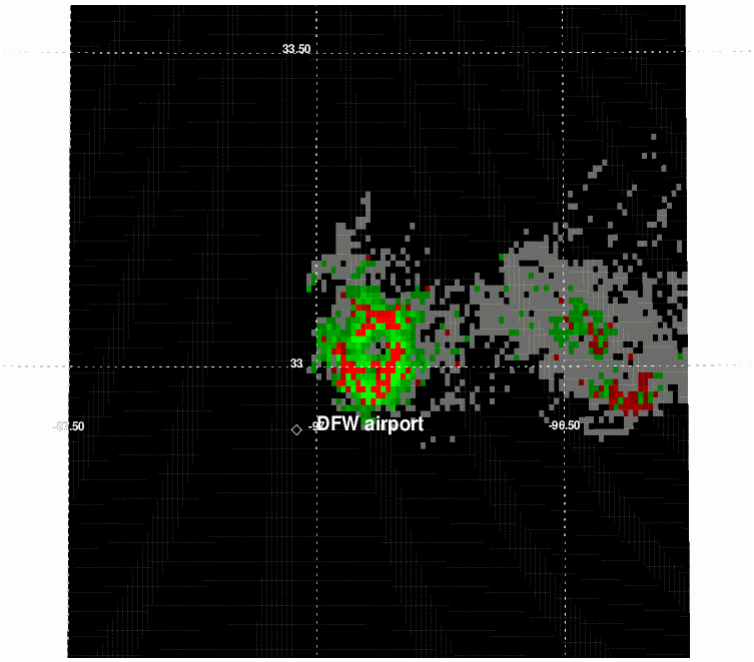

Fig. 8. Same data as in Fig. 7 but plotted to make grid cells that have flash initiation locations stand out. Similar to NEXRAD velocity images, this plot uses green for grid cells that do not have flash initiation locations and red for cells that do. All source densities less than 8 src/km^2/2 min are plotted in gray.

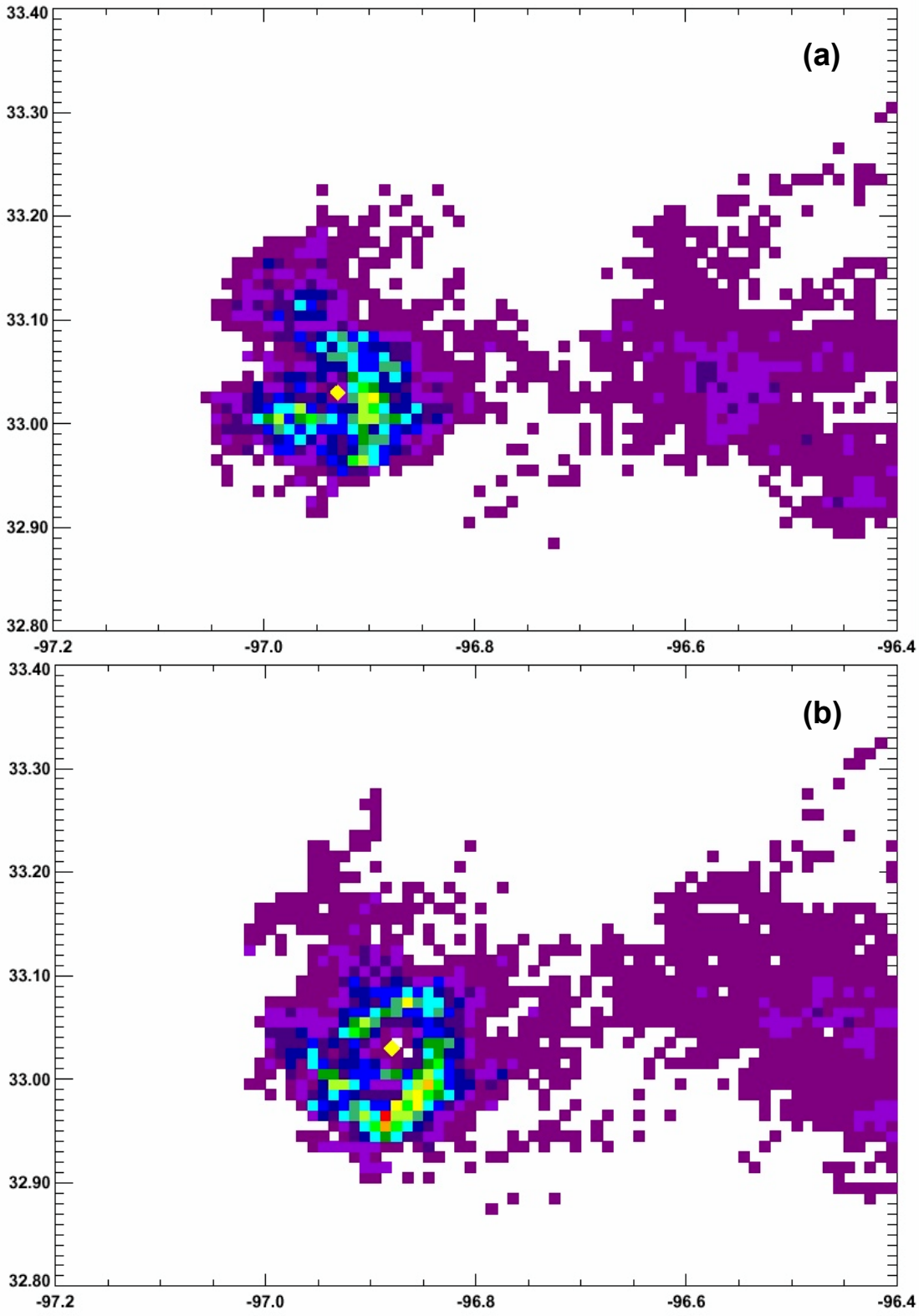

Fig. 9 (a) 1X1-km source density from 0358-0400 Z as a lightning hole (marked by yellow diamond) is breaking up. (b) 1X1-km source density from 0404-0406 Z when new lightning hole dominates storm. Axis numbering shows latitude and longitude.

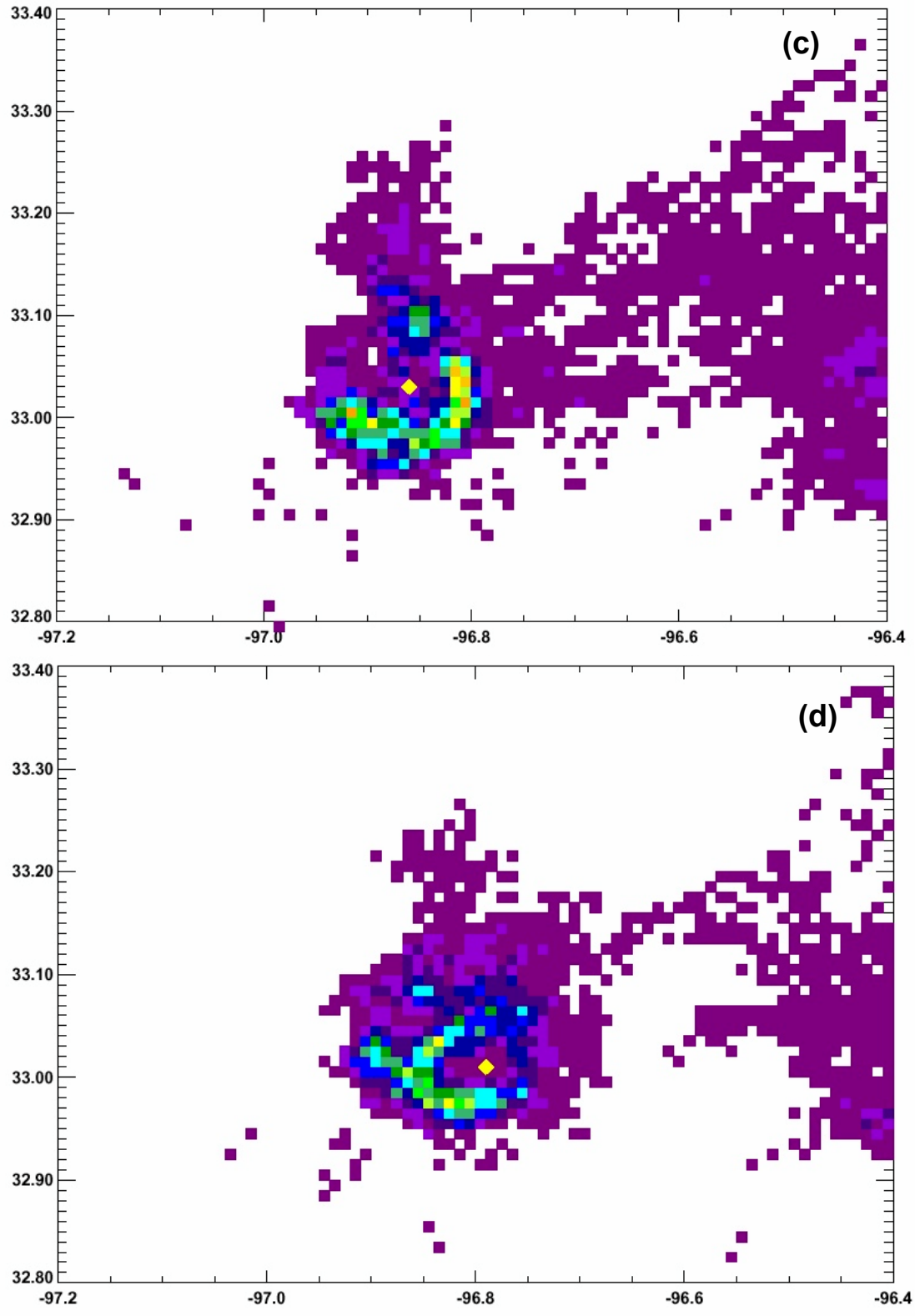

Fig. 9, continued. (c) 1X1-km source density for 0408-0410 Z, as dominant lightning hole from Fig. 9(b) begins to break up. (d) source density for 0412-0414 Z. In (d), previous hole from Figs. 9(b) and 9(c) is still partially open at the west end of the cell as another new hole has formed.

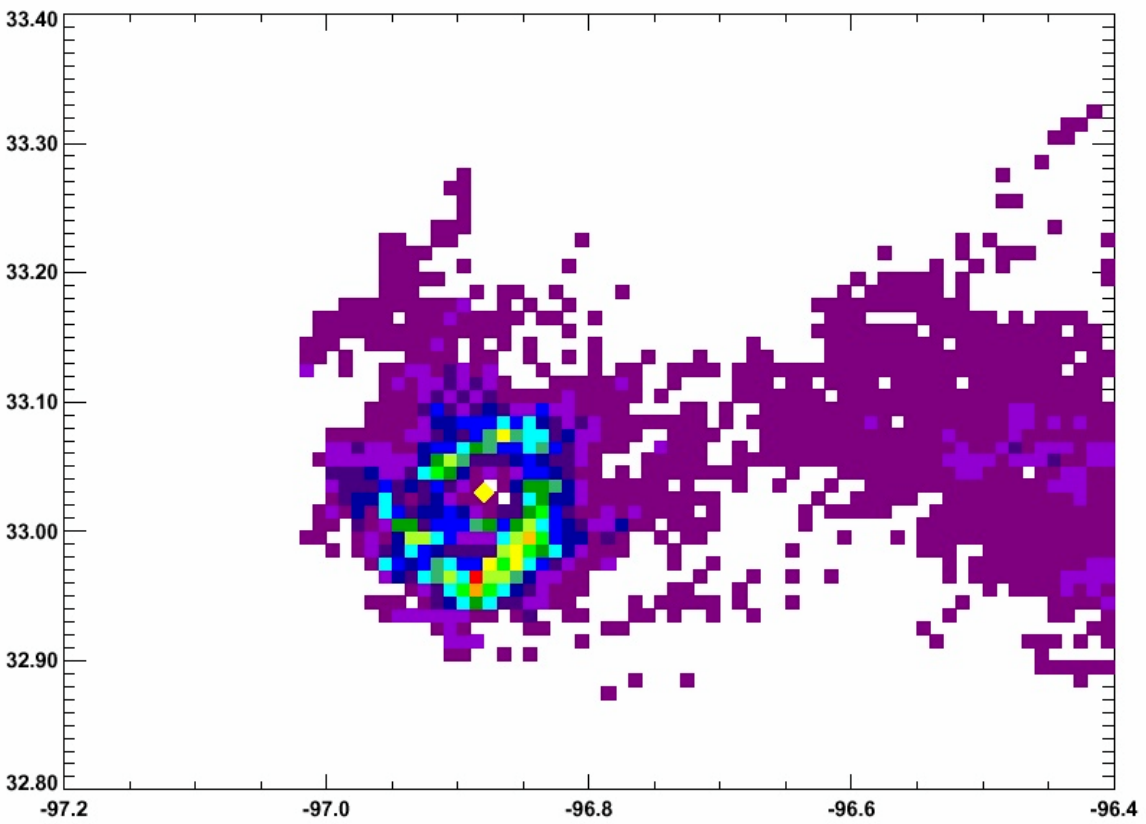

Fig. 10 (a) 1X1 km source density for 0404-0406 Z. A yellow diamond marks the center of the lightning hole.

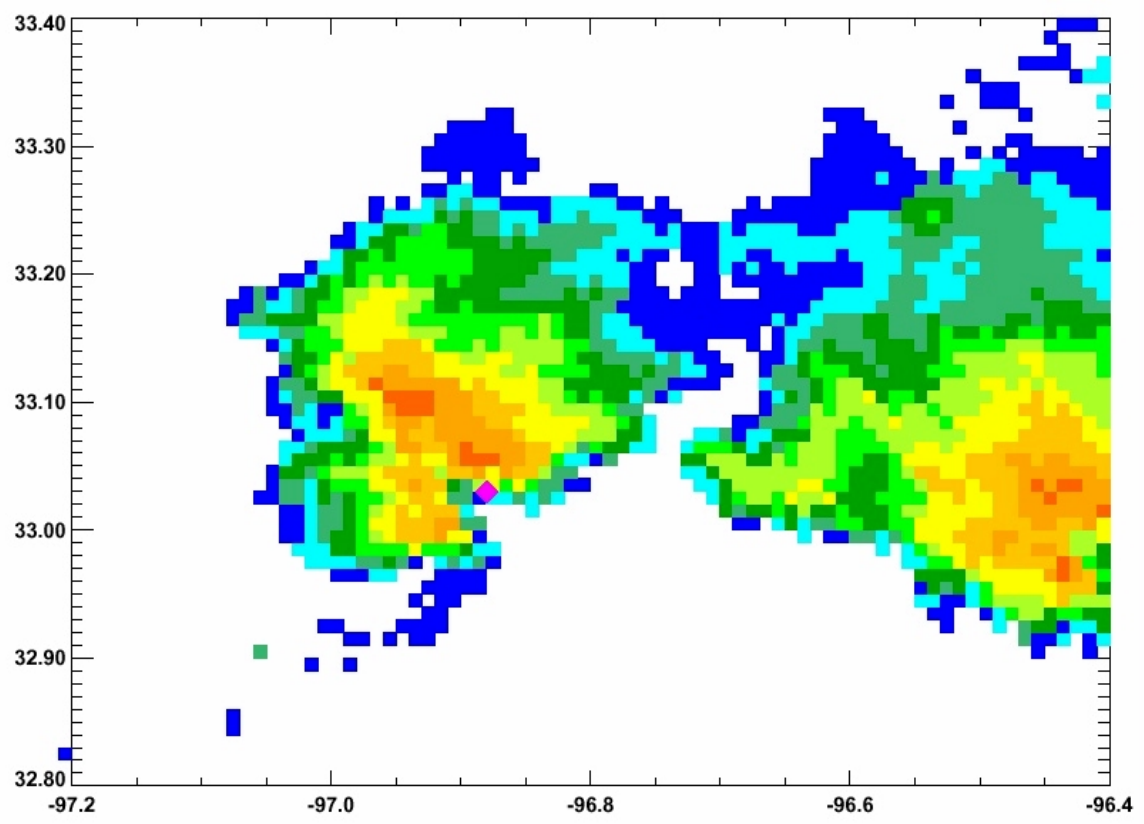

Fig. 10 (b). Base reflectivity at 0405 Z. Values less than 20 dBZ are not plotted; reflectivity color changes every 5 dBZ above 20. Axis numbering shows latitude and longitude. A small pink diamond marks the lightning hole as in Fig 10 (a), showing its spatial relationship to the low-level weak echo region.

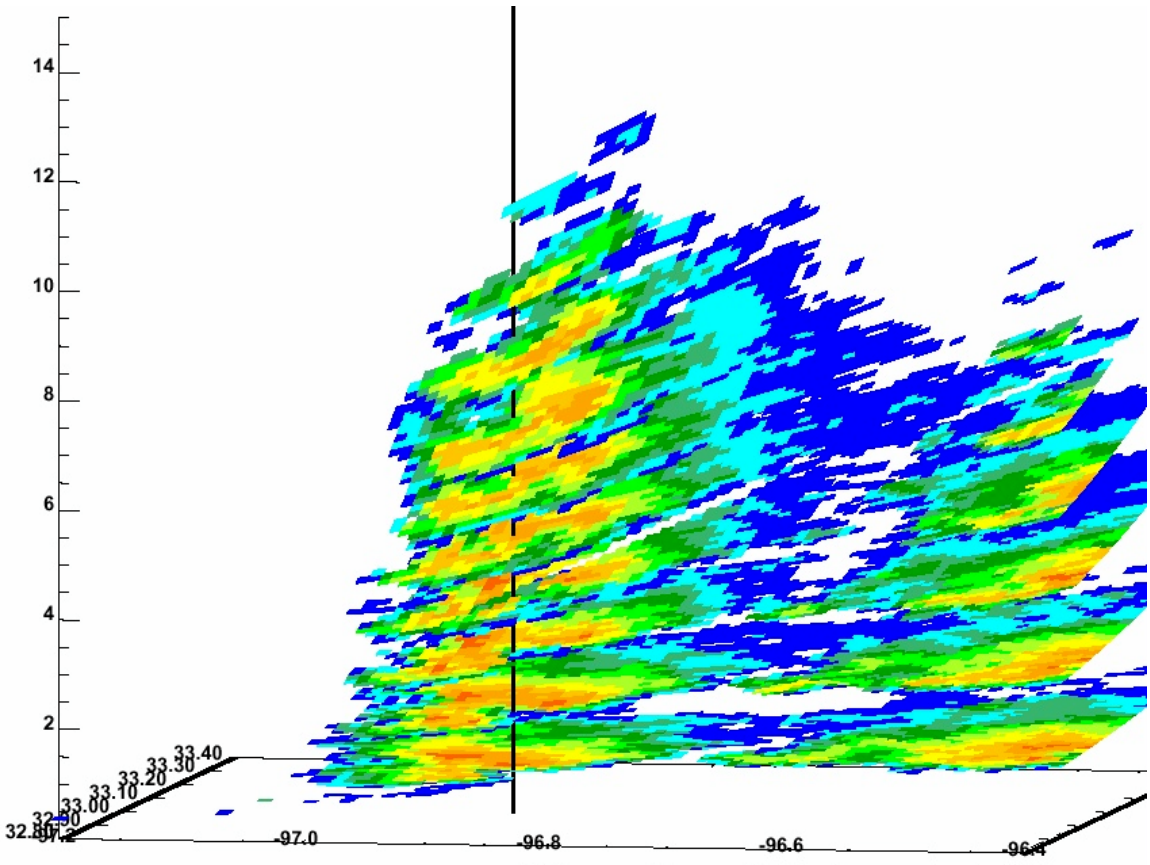

Fig. 10 (c) 3-D view of all tilts of radar volume scan that began at 0405 Z. The position of the lightning hole at 0404Z is marked by a vertical black line (same lat,lon as the pink diamond in Fig. 10(a)). Axis numbering shows latitude and longitude in the horizontal and altitude (in km) on an exaggerated vertical scale. Reflectivities below 20 dBZ are not plotted; reflectivity color changes every 5 dBZ above 20 dBZ.

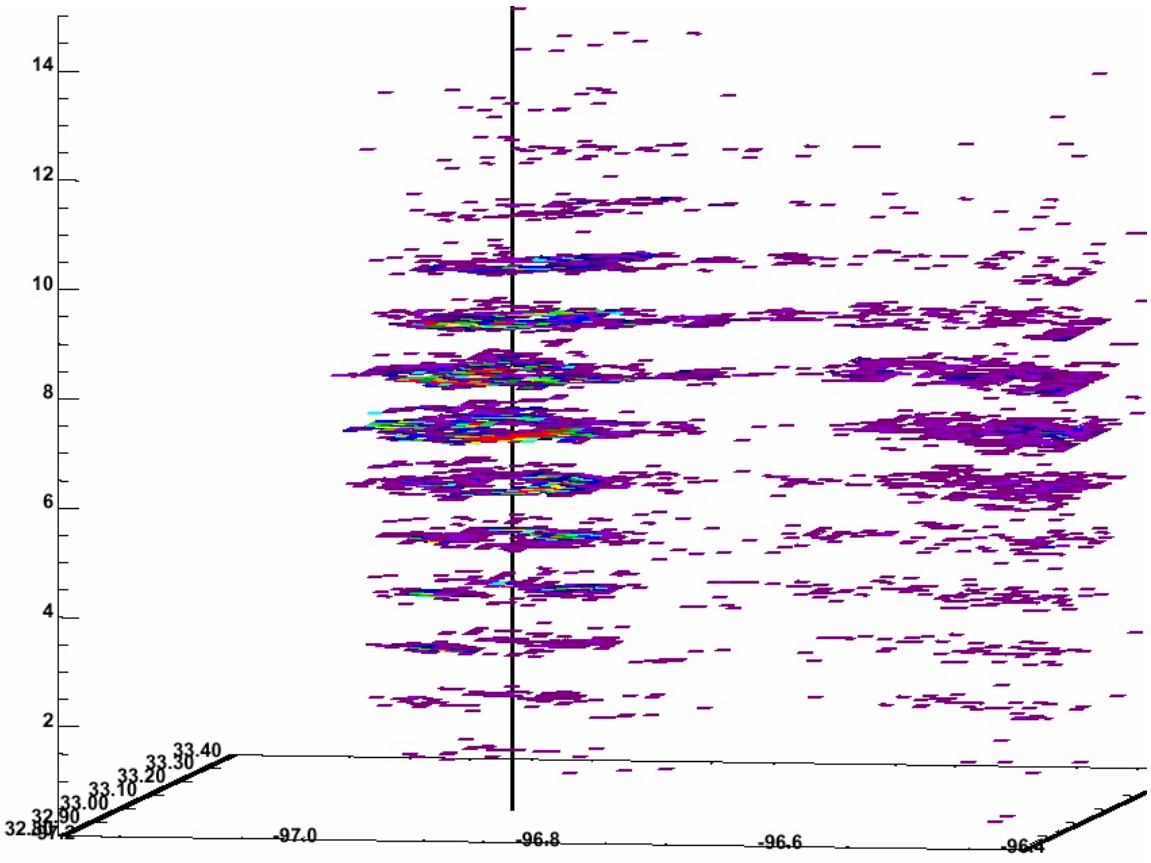

Fig. 10 (d) 1X1 km source density broken into vertical layers, each 1 km thick. Axes and vertical line marking the lightning hole position are the same as in Fig 10 (c).

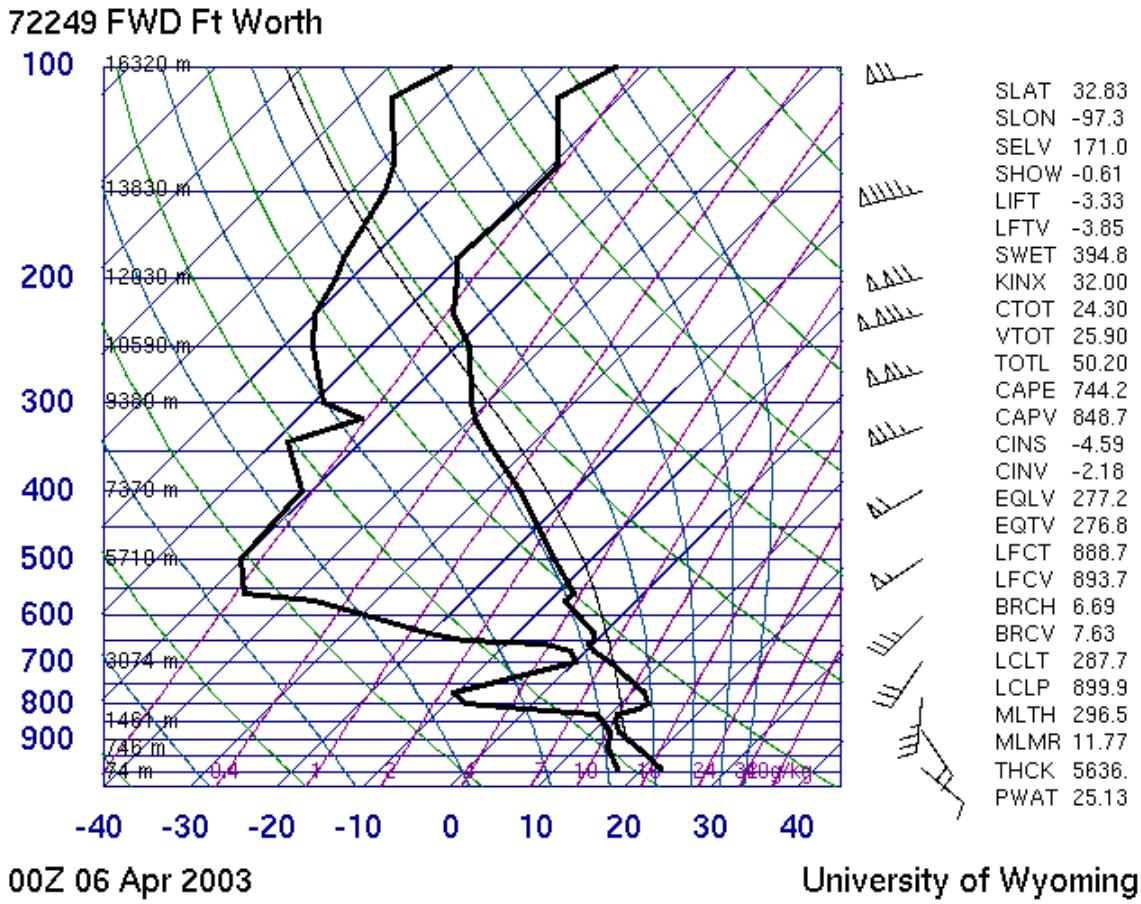

Fig 11. Ft. Worth sounding taken at 0000 Z on April 6, 2003.